FEKO Simulation of Multi-Resonant Low-Profile PIFA

Christian W. Hearn [1] and William A. Davis [2]

[1] Department of Engineering Technology
Weber State University, Ogden, UT 84408-1802, U.S.A.
christianhearn@weber.edu

[2] Department of Electrical and Computer Engineering
Virginia Tech, Blacksburg, VA 24061-011, U.S.A.
WADavis@vt.edu

Abstract **–** A passive, low-profile multi-resonant planar-inverted-F antenna (PIFA) element well-suited for portable communications is presented. The antenna combines the optimal low-profile geometry of a planar inverted-F antenna with a double-tuned structure to create a multi-resonant element with monopole-class radiation properties. The form factor and overall dimensions are held constant for comparisons to a similar single-resonant antenna in different near-field environments.

Index Terms **–** Bandwidth enhancement, double-resonant, low-profile, near-field detuning, PIFA.

I. INTRODUCTION

The planar inverted-F antenna (PIFA) is a popular, small and relatively low-profile, vertically-polarized communications antenna characterized by an omnidirectional radiation pattern in the azimuth (XY) plane. Single-resonant, low-profile configurations of PIFAs suffer from an impedance-bandwidth limitation primarily established by the antenna's effective height. [1].

Double-tuning the PIFA maintains the optimal low-profile characteristic with a potential for increasing impedance bandwidth. The non-volumetric form factor precludes the PIFA from a select class of electrically-small antennas that approach the fundamental limit [2].

However, double-tuning is a useful mechanism to enhance impedance bandwidth in a single frequency band. Comparisons of far-field radiation patterns and mode distributions indicate the radiation properties of the single-resonant and double-tuned PIFAs are nearly equivalent.

One significant fabrication advantage from double-tuning bandwidth enhancement is an effective reduction to near-field detuning prevalent in the integration of small antennas in portable devices.

II. ANTENNA GEOMETRY

The antenna geometry is shown in Fig. 1. The overall height of the antenna is less than one centimeter, which corresponds to an electric height of $h \approx \lambda/35$. The dimensions for the double-tuned PIFA are presented in Table 1. Some miniaturization is achieved with capacitive-loading. Additional miniaturization may be obtained with the introduction of a dielectric. Air-backed dielectrics and perfectly conducting metal are utilized for this example to create a lossless antenna model utilizing FEKO.

The coupling of the driven element to the parasitic element is highly sensitive to both the width and depth of the slot. The vertical shorting bar is common at the base of the PIFA and increases the coupling to the parasitic element. Figure 2 illustrates VSWR impedance responses for the multi-resonant (solid) and single-resonant (dashed) planar inverted-F antennas with similar form-factors. FEKO simulation results shown were with infinite PEC ground planes for matching boundary conditions. Reference impedance for VSWR was *50* Ω. Similar comparisons of VSWR responses for different near-field environments will be presented.

The half-power bandwidths observed from the VSWR responses shown in Fig. 1 are *82 MHz* and *54 MHz* for the multi-resonant and single-resonant elements respectively. The integration of the parasitic element within the same structural form results in a greater than *50%* increase in half-power bandwidth. Differences observed in the radiation pattern and percent power modal distributions are negligible between the multi-resonant and single-resonant models mounted on square ground planes.

Submitted On: December 15, 2014
Accepted On: July 14, 2015

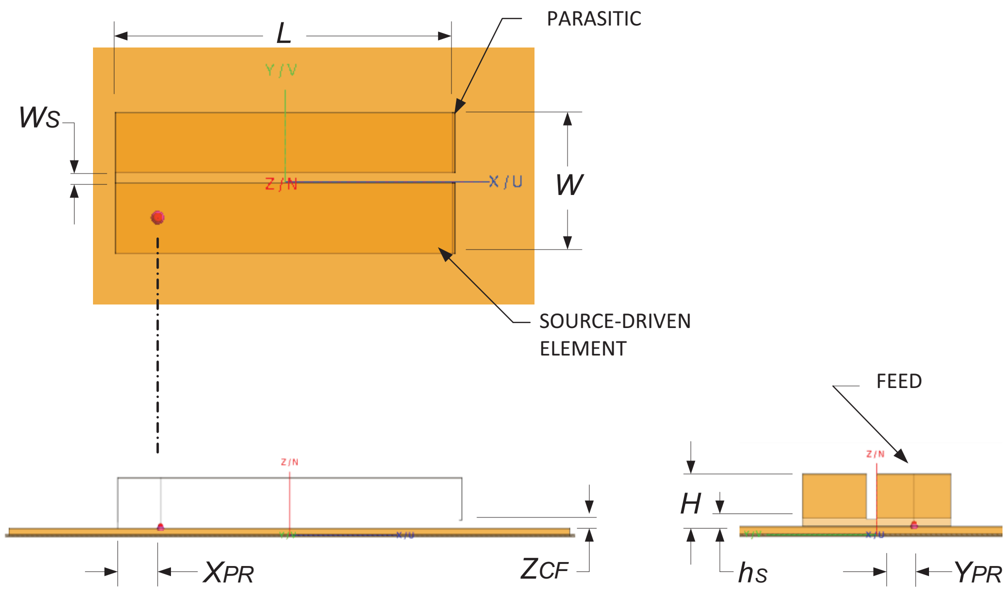

Fig. 1. Engineering perspective of multi-resonant planar inverted-F antenna.

Table 1: Dimensions of the CADFEKO geometry of the multi-resonant PIFA. A capacitive point load of *C=1.65 pF* is applied at the feed for matching

L [cm]	W [cm]	H [cm]	W_S [mm]	h_S [mm]	X_{PR} [mm]	Y_{PR} [mm]	Z_{CF} [mm]
5.52	2.29	0.83	1.65	1.10	7.0	5.7	1.4

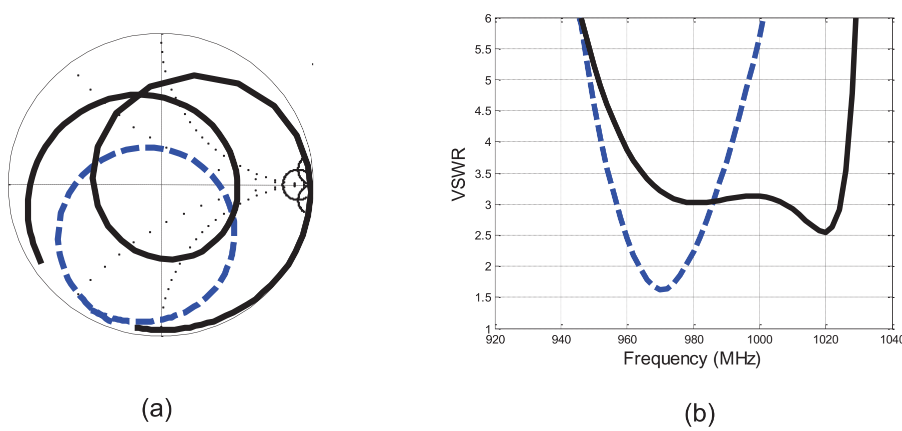

Fig. 2. (a) Normalized impedance and (b) VSWR responses for multi-resonant (solid) and single-resonant (dashed) planar inverted-F antennas with similar form-factors. The boundary condition for both simulations shown was a perfect-electrically-conducting (PEC) infinite ground plane.

III. ANTENNA GEOMETRY

The multi-resonant PIFA was mounted on a PEC model of a handheld chassis to assess the antenna sensitivity to a typical near-field environment. Single-resonant monopole-class antennas are typically less sensitive to antenna placement/structure interaction, where multi-resonant low-profile antennas may suffer significant detuning with a similar change in boundary conditions.

The purpose of the step is to determine if the multi-resonant PIFA maintains the double-tuning impedance characteristic and omnidirectional radiation in azimuth when subjected to a different boundary condition and near-field environment.

Figure 3 illustrates the integration of the double-resonant PIFA to a handheld device platform. The dimensions of the lossless chassis are approximately *H=10 cm*, *W=6.5 cm* and *D=4.0 cm.*

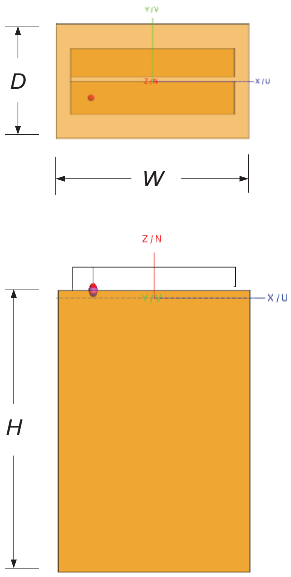

Fig. 3. CADFEKO rendering of double-resonant PIFA integrated to handheld device platform. The dimensions of the lossless chassis are approximately *H=10 cm*, *W=6.5 cm* and *D=4.0 cm*.

Tuning of the multi-resonant PIFA on the handheld chassis can be improved with adjustments to the coupling factors (slot width, W_s, and the depth of the slot on the shorting bar, h_s). Table 2 indicates changes to the two coupling parameters. The PIFA form factor and probe position are held constant. The same capacitive point load (*C=1.65 pF*) is applied at the feed for matching.

Table 2: Tuning parameters for integration of double-resonant PIFA to the portable structure (shown in Fig. 3). PIFA geometry and probe position are held constant. The same capacitive point load (*C=1.65 pF*) is applied at the feed for matching

Double-Resonant PIFA	W_S [mm]	h_S [mm]
Un-tuned	1.65	1.1
Tuned	0.70	4.4

Figure 4 compares the VSWR responses of the un-tuned and tuned double-resonant PIFAs integrated to a handheld device. The infinite ground plane model (described in Fig. 1 and Table 1) was directly applied to the handheld device. No adjustments to coupling factors and/or probe position were made for the dashed trace. The double-tuning characteristic was maintained from a change in boundary conditions without tuning.

The solid trace incorporates the slot parameter adjustments shown in Table 2. The observed result is an increase in 2:1 impedance bandwidth of *ΔB≈25%.*

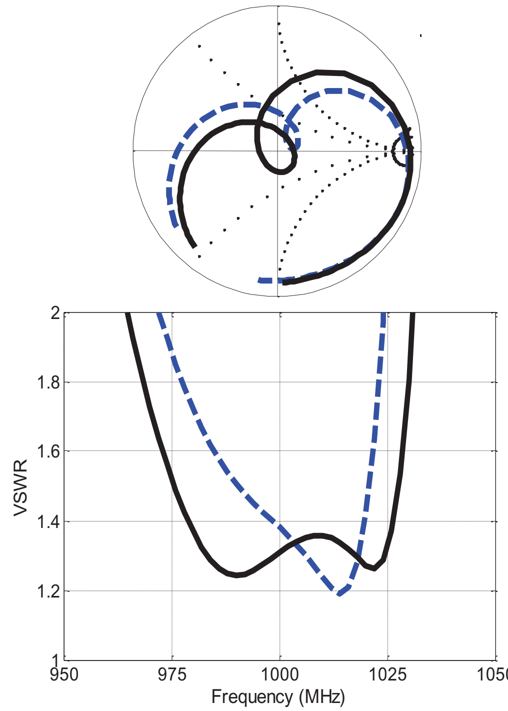

Fig. 4. Impedance responses for 'untuned' (dashed) and 'tuned' (solid) double-resonant PIFAs integrated to a handheld device (shown in Fig. 3). The observed results are the double-tuning is maintained but with adjustments to the parameters of the coupling slot, an increase in 2:1 VSWR impedance bandwidth of *ΔB≈25%* may be obtained.

Figure 5 (a) presents the normalized impedance and (b) VSWR responses for the single resonant (dashed) double-resonant (solid) inverted-F antennas mounted on the handheld chassis. The 2:1 VSWR bandwidths for the single-resonant and tuned double-resonant antennas are *46 MHz* and *65 MHz* respectively. The double-tuning seen clearly in Fig. 5 (a) results in a 2:1 VSWR impedance bandwidth improvement of greater than *ΔB>40%*.

Figure 6 (a) presents the E_θ and (b) E_Φ radiation patterns for the multi-resonant PIFA mounted on a handheld chassis. The significant coupling between the source-driven element and the parasitic creates nearly symmetric patterns with negligible differences in comparison to the single resonant PIFA mounted to the same chassis.

Figure 7 (a-d) are post-processed renderings of the surface current distributions of the multi-resonant PIFA mounted on the handheld chassis. The magnitudes of the surface current densities for both the driven and parasitic elements are comparable. Some phasing is observed at ωt=[0°,180°] where the currents on the parasitic element are lagging the driven element currents.

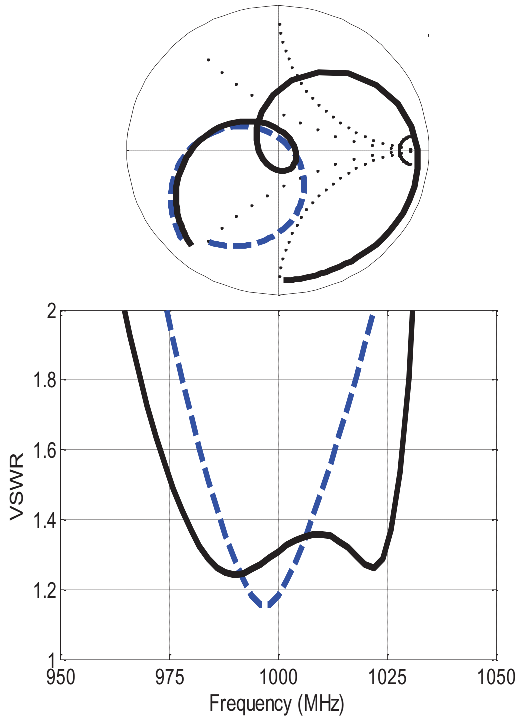

Fig. 5. (a) Normalized impedance and (b) VSWR for the double resonant (solid) and single-resonant (dashed) PIFA integrated to handheld device (shown in Fig. 3).

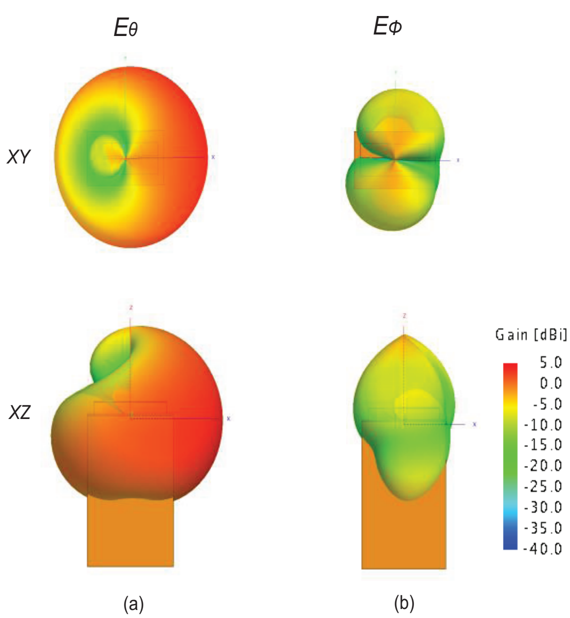

Fig. 6. POSTFEKO renderings of:(a) E_θ and (b) E_Φ radiation patterns for the multi-resonant PIFA mounted on a handheld chassis.

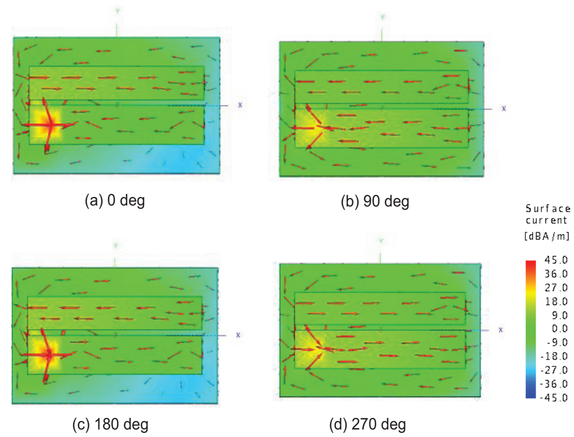

Fig. 7. Surface current distributions on handheld PIFA geometry for ωt=[0°,90°,180°,270°].

IV. DISCUSSION

The double-tuned PIFA shown in Fig. 3 enhanced the impedance bandwidth in a single frequency band. Figure 4 illustrates an effective reduction to near-field detuning prevalent in the integration of small antennas in portable devices. The position of the probe and parameters of the slot were unchanged from the finite ground plane example shown earlier. The result indicates the double-tuning characteristic is maintained with the change in finite ground plane/near-field environment of the radiating structure.

Both the source-driven and parasitic elements share part of the shorting bar to increase coupling. The increased coupling balances the surface current distributions and minimizes asymmetries in the far-field radiation patterns.

Bandwidth performance beyond double-tuning and multi-resonant techniques for antenna designs can be improved with the reduction of sharp edges, mechanically in the structural design of the antenna [3], and electrically, in terms of reducing the slope discontinuities in the surface current distributions [4].

V. CONCLUSION

A passive, low-profile multi-resonant antenna element with monopole radiation characteristics has been introduced. The structure is an extension of the planar inverted-F antenna with a double-tuned structure to enhance reliable operation in unknown environments. The overall height of the antenna is less than one centimeter, which corresponds to an electric height of $h \approx \lambda/35$.

Comparisons to a similar low-profile single-resonant antenna in both the finite ground plane and handheld geometries were shown. The source-driven element and parasitic are joined at the base of the shorting bar to improve the capacitive coupling. The result is a balanced element in terms of radiation and modal performance with a double-tuned impedance response and 2:1 VSWR bandwidth improvement of over forty percent.

REFERENCES

[1] L. M. Feldner, et. al., “Electrically-small frequency-agile PIFA-as-a-package for portable wireless devices,” *IEEE Trans. Antennas Propagat.*, vol. 55, no. 11, pp. 3310-3319, Nov. 2007.

[2] L. J. Chu, “Physical limitations of omni-directional antennas,” *J. Appl. Phys*., vol. 19, pp. 1163-1175, Dec. 1948.

[3] D. F. Sievenpiper, et. al., “Experimental validation of performance limits and design guidelines for small antennas,” *IEEE Trans. Antennas Propagat.*, vol. 60, no. 1, pp. 8-19, Jan. 2012.

[4] T. Yang, et. al., “Cellular-phone and hearing-aid. Interaction: an antenna solution,” *IEEE Antennas and Propagation Magazine*, vol. 50, no. 3, pp. 51-64, June 2008.

Christian Hearn received the Ph.D. degree from Virginia Polytechnic Institute and State University in 2012. He was a Member of the Virginia Tech Antenna Group and a Research Engineer for Applied EM during his Ph.D. plan-of-study. He was originally a Mechanical Engineer for NSWC-UERD and earned a professional engineering license before returning to graduate school in Electrical Engineering. Hearn is currently an Assistant Professor at Weber State University, College of Applied Science and Technology. His interests are design and validation of multi-resonant electrically-small antennas, in addition to communications and signal processing.

William A. Davis received the Ph.D. degree from the University of Illinois, Urbana in 1974. He has held academic positions at both the Air Force Institute of Technology and Virginia Polytechnic Institute and State University, Blacksburg where he is a Professor Emeritus and Director of the Virginia Tech Antenna Group. His primary interests are antennas, measurements, scattering theory and material characterization with an emphasis on numerical method, electromagnetic theory and microwave measurements.